

LONGITUDINAL IMPEDANCE OF SIMPLE CYLINDRICALLY SYMMETRIC STRUCTURES\*

S. KHEIFETS

Stanford Linear Accelerator Center, Stanford University, Stanford, California 94305

ABSTRACT

A method derived<sup>1</sup> for calculation of electromagnetic fields of a point charge moving along an axis of cylindrically symmetric structures is applied here to cavities and collimators with side tubes. The longitudinal impedance for such structures is calculated. In particular, the impedance for a pipe loaded with a thin washer is also calculated. It is shown that for large particle energy and for high frequencies the longitudinal impedance of a collimator can be found analytically and that it is a constant in a broad range of frequencies.

1. INTRODUCTION

A method of calculating electromagnetic (EM) fields excited by a point charge  $Q$  moving with a constant velocity  $u$  along the axis of a cylindrical perfectly conducting pipe with an abrupt change in its cross section was developed and published recently.<sup>1</sup> This method can be generalized to make it applicable to any cylindrically symmetric metallic structures that can be cut orthogonal to the axis of symmetry into a number of regions such that within each region cross sections are identical. Regions supposed to be electrically connected to each other. Each region can be bounded by one or several coaxial metallic cylindrical surfaces.

In essence, the generalized method consists of three steps. First, the Fourier components of the EM fields in each region are expanded into series of cylindrical waves. Each wave satisfies the boundary conditions on the cylindrical metallic surfaces. The series still contain an infinite number of yet unknown coefficients. Second, continuity and additional boundary conditions are imposed on the EM field at each cross sectional interface between different regions (field matching). Third, the resulting transcendental equations are transformed into an infinite set of linear algebraic equations for the expansion coefficients. The approximate solution of the algebraic set of equations is then obtained numerically by truncating it. Physically interesting quantities, for example, the fields and the longitudinal coupling impedance, are expressed in terms of these coefficients.

In the present paper this method is applied to a case of a point charge moving along the axis of either of the two structures sketched in Figs. 1a (a cylindrical cavity with side pipes) and 1b (a cylindrical collimator). The longitudinal impedances for such structures are calculated. The results found here for a cavity with the side pipes of equal cross sections are compared with calculations performed by another method of matching fields on the cylindrical surface  $r = a$ .<sup>2</sup> This comparison shows good agreement.

There is a certain advantage in matching fields on the interfaces  $z = \text{constant}$  rather than on the interfaces  $r = \text{constant}$ . First, it lets one consider structures with indentations. Next, the two side pipes can have different radii. The method presented allows one to take this case into account practically without any additional complications. It is also straightforward to extend the method to the case of a charge moving off the axis to find the transverse impedance.

Some other practically interesting structures are particular cases of geometries considered here. One example is a cylindrical pipe loaded with a washer. Another example considered here is a flange connection of two tubes which in the presence of a vacuum edge may form a very thin cylindrical cavity.

\* Work supported by the Department of Energy, contract DE-AC03-76SF00515.

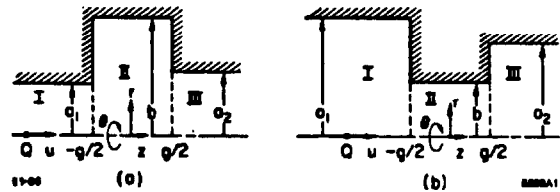


Fig. 1. Cylindrically symmetric structures considered in the present work: a) Cavity and b) Collimator of the radius  $b$  and the length  $g$  with side pipes of the radii  $a_1$  and  $a_2$ .

Two geometries considered in Ref. 1 (a pipe with a sudden increase or decrease of its cross section) are also particular cases of geometries considered in the present paper.

Of particular interest is the question of the behavior of the impedance for very high frequencies. For the case of a collimator the asymptotic behavior of the impedance can be calculated analytically. This calculation can be found in the Appendix. Under the assumptions made in the present work, the impedance is independent of the frequency and is equal to  $120 \ln(a/b) \Omega$ , where  $a$  is the cross section radius of the pipe at the exit of the indentation.

The equations derived here are valid for any particle velocity  $\beta = u/c$ , with  $c$  the speed of light. Thus one can solve for fields radiated by a charge with an arbitrary energy. A note of caution is appropriate here. For very low  $\beta$  the assumption that velocity is constant *does not* hold. In that case the problem should be solved self-consistently, as was done for example in the paper.<sup>3</sup> A relativistic case can be easily obtained by assuming  $\gamma \gg 1$ , where  $\gamma$  is the Lorentz factor of the charge. Most results obtained here are pertinent for large  $\gamma$ .

Throughout this paper the right-hand cylindrical coordinate system  $r, \theta, z$  is used. The current density of a point charge moving along the axis of the pipe is

$$\mathbf{j} = \mathbf{e}_r 0 + \mathbf{e}_\theta 0 + \mathbf{e}_z \frac{Qu}{2\pi r} \delta(r) \delta(z - ut) \quad (1.1)$$

where  $\delta(x)$  is Dirac's  $\delta$ -function. If one defines the Fourier components of any vector  $\mathbf{V}$  for the angular frequency  $\omega$  by expression

$$\tilde{\mathbf{V}} = \frac{1}{2\pi} \int_{-\infty}^{+\infty} dt \mathbf{V} \exp\{i\omega t\} \quad (1.2)$$

then the Fourier components of the current density is

$$\tilde{\mathbf{j}} = \mathbf{e}_r 0 + \mathbf{e}_\theta 0 + \mathbf{e}_z \frac{Q\delta(r)}{2\pi r} \exp\{i\omega z/u\} \quad (1.3)$$

2. Field Expansions

Using well-known expressions for the EM fields of a point charge moving along the axis of a cylindrical pipe<sup>4</sup> and for eigenfunctions of a pipe,<sup>5</sup> it is easy to represent the EM field components for any region shown in Fig. 1 as an expansion into series of the cylindrical waves with unknown coefficients (see, e.g., Ref. 1). Let us introduce the following notation:

$$k = \omega/c \quad , \quad (2.1)$$

$$\tau = k/\beta\gamma \quad , \quad (2.2)$$

$$M = Qk/\pi c\gamma^2\beta^2 \quad , \quad (2.3)$$

$$G_1(r, d) = K_1(\tau r) + I_1(\tau r)K_0(\tau d)/I_0(\tau d) \quad , \quad (2.4)$$

$$G_0(r, d) = K_0(\tau r) - I_0(\tau r)K_0(\tau d)/I_0(\tau d) \quad , \quad (2.5)$$

where  $d = a_1, a_2$  or  $b$ ,  $K_0, K_1, I_0$  and  $I_1$  are modified Bessel functions of the second and the first kind, and the zeroth and the first order, respectively.

Then for the diffraction region  $z > g/2$  (Region III in Fig. 1) we have:

$$\begin{aligned} \tilde{E}_r^+ &= \gamma M G_1(r, a_2) \exp\{ikz/\beta\} - i \Sigma_n B_n^+(\nu_n/a_2) \\ & J_1(\nu_n r/a_2) \lambda_{a_2 n} \exp\{iz\lambda_{a_2 n}\} \quad , \quad (2.6) \end{aligned}$$

$$\begin{aligned} \tilde{E}_z^+ &= -i M G_0(r, a_2) \exp\{ikz/\beta\} + \Sigma_n B_n^+(\nu_n^2/a_2^2) \\ & J_0(\nu_n r/a_2) \exp\{iz\lambda_{a_2 n}\} \quad , \quad (2.7) \end{aligned}$$

$$\begin{aligned} \tilde{H}_\theta^+ &= \gamma \beta M G_1(r, a_2) \exp\{ikz/\beta\} - ik \Sigma_n B_n^+(\nu_n/a_2) \\ & J_1(\nu_n r/a_2) \exp\{iz\lambda_{a_2 n}\} \quad , \quad (2.8) \end{aligned}$$

where  $\lambda_{a_2 n} = \sqrt{k^2 - \nu_n^2/a_2^2}$  and  $J_0, J_1$  are Bessel functions of the first kind, of the zeroth and the first order, respectively.

Similarly, for the reflection region  $z < -g/2$  (Region I in Fig. 1) we have:

$$\begin{aligned} \tilde{E}_r^- &= \gamma M G_1(r, a_1) \exp\{ikz/\beta\} + i \Sigma_n B_n^-(\nu_n/a_1) \\ & J_1(\nu_n r/a_1) \lambda_{a_1 n} \exp\{-iz\lambda_{a_1 n}\} \quad , \quad (2.9) \end{aligned}$$

$$\begin{aligned} \tilde{E}_z^- &= -i M G_0(r, a_1) \exp\{ikz/\beta\} + \Sigma_n B_n^-(\nu_n^2/a_1^2) \\ & J_0(\nu_n r/a_1) \exp\{-iz\lambda_{a_1 n}\} \quad , \quad (2.10) \end{aligned}$$

$$\begin{aligned} \tilde{H}_\theta^- &= \gamma \beta M G_1(r, a_1) \exp\{ikz/\beta\} - ik \Sigma_n B_n^-(\nu_n/a_1) \\ & J_1(\nu_n r/a_1) \exp\{-iz\lambda_{a_1 n}\} \quad , \quad (2.11) \end{aligned}$$

where  $\lambda_{a_1 n} = \sqrt{k^2 - \nu_n^2/a_1^2}$ .

Finally, for the intermediate region  $-g/2 < z < g/2$  (Region II in Fig. 1) we have:

$$\begin{aligned} \tilde{E}_r^0 &= \gamma M G_1(r, b) \exp\{ikz/\beta\} - i \Sigma_n (\nu_n/b) \\ & J_1(\nu_n r/b) \lambda_{bn} (C^+ \exp\{iz\lambda_{bn}\} - C^- \exp\{-iz\lambda_{bn}\}) \quad , \quad (2.12) \end{aligned}$$

$$\begin{aligned} \tilde{E}_z^0 &= -i M G_0(r, b) \exp\{ikz/\beta\} + \Sigma_n (\nu_n^2/b^2) \\ & J_0(\nu_n r/b) (C^+ \exp\{iz\lambda_{bn}\} + C^- \exp\{-iz\lambda_{bn}\}) \quad , \quad (2.13) \end{aligned}$$

$$\begin{aligned} \tilde{H}_\theta^0 &= \gamma \beta M G_1(r, b) \exp\{ikz/\beta\} - ik \Sigma_n (\nu_n/b) \\ & J_1(\nu_n r/b) (C^+ \exp\{iz\lambda_{bn}\} + C^- \exp\{-iz\lambda_{bn}\}) \quad , \quad (2.14) \end{aligned}$$

where  $\lambda_{bn} = \sqrt{k^2 - \nu_n^2/b^2}$ .

All the other field components are zero due to cylindrical symmetry of the problem.

The eigenvalues  $\nu_n$  are defined by the boundary condition  $E_z(z) = 0$  for  $r = d$  which gives the following formula for  $\nu_n$ :

$$J_0(\nu_n) = 0, \quad n = 1, 2, \dots, \infty \quad . \quad (2.15)$$

They are assumed to be arranged in ascending order:  $\nu_1 < \nu_2 < \dots < \infty$ . In all field expansions above,  $B_n^\pm$  and  $C^\pm$  are unknown coefficients to be defined by the boundary and continuity conditions on the interfaces  $z = \text{constant}$  between adjacent cylindrical regions.

To ascertain the proper asymptotic behavior of the diffracted field for  $z \rightarrow \infty$  and the reflected field for  $z \rightarrow -\infty$  the imaginary parts of the propagation constants should be chosen positive (such a choice is known as the radiation condition):

$$\text{Im} \lambda_{a_1 n} > 0 \quad , \quad (2.16)$$

$$\text{Im} \lambda_{a_2 n} > 0 \quad . \quad (2.17)$$

The same sign is chosen for the propagation constant in the Region II:

$$\text{Im} \lambda_{bn} > 0 \quad . \quad (2.18)$$

Each term in expressions (2.6-2.8) for the diffracted field describes either the  $n^{\text{th}}$  wave propagating in the positive  $z$  direction, if  $k > \nu_n/a_2$ , or an evanescent wave, if  $k < \nu_n/a_2$ . Similarly, each term in expressions (2.9-2.11) for the reflected field describes either the  $n^{\text{th}}$  wave propagating in the negative  $z$  direction, if  $k > \nu_n/a_1$ , or an evanescent wave, if  $k < \nu_n/a_1$ . For any given  $k$  there are a finite number of propagating and an infinite number of evanescent waves.

### 3. Boundary and Continuity Conditions

The expansions of the EM fields given in the previous section are constructed in such a way as to fulfill the boundary conditions on the wall of the pipe in any region with a constant pipe radius. For example, for  $r = a_2$  and for all  $z > g/2$ ,

$$\tilde{E}_z^+(z) = 0 \quad . \quad (3.1)$$

Consider now an interface between two regions. In the plane of the interface:

- the radial component of the electric field on the inner side of the wall should be equal to zero for all  $r$ ,
- all three components of the field should be continuous across the opening.

For example, for a cavity at  $z = g/2$ ,

$$\tilde{E}_r^0(r) = 0 \quad \text{for all } a_2 < r < b \quad , \quad (3.2)$$

and for all  $r < a_2$ ,

$$\tilde{E}_z^+(r) = \tilde{E}_z^0(r) \quad , \quad (3.3)$$

$$\tilde{H}_\theta^+(r) = \tilde{H}_\theta^0(r) \quad , \quad (3.4)$$

$$\tilde{E}_r^+(r) = \tilde{E}_r^0(r) \quad . \quad (3.5)$$

Analogous expressions can be written for another cavity interface  $z = -g/2$  and for a collimator. It is well-known that one of the three conditions (3.3-3.5) is always fulfilled as soon as two others of them are fulfilled. In what follows continuity conditions for  $E_r$  and  $E_z$  are chosen to determine unknown expansion coefficients.

We introduce now the dimensionless variables:

$$\kappa = kb \quad , \quad (3.6)$$

$$p_1 = 1/q_1 = a_1/b \quad , \quad (3.7)$$

$$p_2 = 1/q_2 = a_2/b \quad , \quad (3.8)$$

$$\tilde{g} = g/2b \quad , \quad (3.9)$$

$$\rho = r/b \quad . \quad (3.10)$$

In these variables the propagation constants are

$$\tilde{\lambda}_{a1n} = \lambda_{a1n}b = \sqrt{\kappa^2 - \nu_n^2/p_1^2}, \quad (3.11)$$

$$\tilde{\lambda}_{a2n} = \lambda_{a2n}b = \sqrt{\kappa^2 - \nu_n^2/p_2^2}, \quad (3.12)$$

$$\tilde{\lambda}_{bn} = \lambda_{bn}b = \sqrt{\kappa^2 - \nu_n^2}. \quad (3.13)$$

It is also useful to redefine the expansion coefficients

$$B_n^- = -(2ibQ/\pi c) \exp\{-i\tilde{g}(\kappa/\beta + \tilde{\lambda}_{a1n})\}x_n, \quad (3.14)$$

$$C_n^- = -(2ibQ/\pi c) \exp\{+i\tilde{g}(\kappa/\beta + \tilde{\lambda}_{bn})\}t_n, \quad (3.15)$$

$$C_n^+ = -(2ibQ/\pi c) \exp\{-i\tilde{g}(\kappa/\beta - \tilde{\lambda}_{bn})\}y_n, \quad (3.16)$$

$$B_n^+ = +(2ibQ/\pi c) \exp\{+i\tilde{g}(\kappa/\beta - \tilde{\lambda}_{a2n})\}z_n. \quad (3.17)$$

The expressions for the field components in the plane  $z = -g/2$  in these variables become:

$$\begin{aligned} \tilde{E}_r^- &= (2Q/\pi cb) \exp\{-i\kappa\tilde{g}/\beta\}[(\kappa/2\gamma\beta^2)G_1(r, a_1) \\ &+ (1/p_1)\Sigma_n x_n \nu_n J_1(\nu_n \rho/p_1)\tilde{\lambda}_{a1n}] \end{aligned} \quad (3.18)$$

$$\begin{aligned} \tilde{E}_r^0 &= (2Q/\pi cb) \exp\{-i\kappa\tilde{g}/\beta\}[(\kappa/2\gamma\beta^2)G_1(r, b) \\ &+ \Sigma_n \nu_n J_1(\nu_n \rho)\tilde{\lambda}_{bn}(t_n \exp\{2i\tilde{g}(\kappa/\beta + \tilde{\lambda}_{bn}) - y_n\})] \end{aligned} \quad (3.19)$$

$$\begin{aligned} \tilde{E}_z^- &= -(2iQ/\pi cb) \exp\{-i\kappa\tilde{g}/\beta\}[(\kappa/2\gamma^2\beta^2)G_0(r, a_1) \\ &+ (1/p_1^2)\Sigma_n x_n \nu_n^2 J_0(\nu_n \rho/p_1)] \end{aligned} \quad (3.20)$$

$$\begin{aligned} \tilde{E}_z^0 &= -(2iQ/\pi cb) \exp\{-i\kappa\tilde{g}/\beta\}[(\kappa/2\gamma^2\beta^2)G_0(r, b) \\ &+ \Sigma_n \nu_n^2 J_0(\nu_n \rho)(t_n \exp\{2i\tilde{g}(\kappa/\beta + \tilde{\lambda}_{bn}) + y_n\})] \end{aligned} \quad (3.21)$$

Similar expressions for the field components in the plane  $z = g/2$  are

$$\begin{aligned} \tilde{E}_r^+ &= (2Q/\pi cb) \exp\{i\kappa\tilde{g}/\beta\}[(\kappa/2\gamma\beta^2)G_1(r, a_2) \\ &+ (1/p_2)\Sigma_n z_n \nu_n J_1(\nu_n \rho/p_2)\tilde{\lambda}_{a2n}] \end{aligned} \quad (3.22)$$

$$\begin{aligned} \tilde{E}_r^0 &= (2Q/\pi cb) \exp\{i\kappa\tilde{g}/\beta\}[(\kappa/2\gamma\beta^2)G_1(r, b) \\ &+ \Sigma_n \nu_n J_1(\nu_n \rho)\tilde{\lambda}_{bn}(t_n - y_n \exp\{-2i\tilde{g}(\kappa/\beta - \tilde{\lambda}_{bn})\})] \end{aligned} \quad (3.23)$$

$$\begin{aligned} \tilde{E}_z^+ &= -(2iQ/\pi cb) \exp\{i\kappa\tilde{g}/\beta\}[(\kappa/2\gamma^2\beta^2)G_0(r, a_2) \\ &- (1/p_2^2)\Sigma_n z_n \nu_n^2 J_0(\nu_n \rho/p_2)] \end{aligned} \quad (3.24)$$

$$\begin{aligned} \tilde{E}_z^0 &= -(2iQ/\pi cb) \exp\{i\kappa\tilde{g}/\beta\}[(\kappa/2\gamma^2\beta^2)G_0(r, b) \\ &+ \Sigma_n \nu_n^2 J_0(\nu_n \rho)(t_n + y_n \exp\{-2i\tilde{g}(\kappa/\beta + \tilde{\lambda}_{bn})\})] \end{aligned} \quad (3.25)$$

Note that these expressions are valid both for a cavity, for which  $p_1 < 1$  and  $p_2 < 1$ , and for a collimator, for which  $p_1 > 1$  and  $p_2 > 1$ .

#### 4. Basic Equations

Unknown coefficients  $x_n, y_n, t_n$  and  $z_n$  are defined by the set of equations which are obtained by substituting expressions (3.18) through (3.25) into Eqs. (3.2) through (3.5) for the interface  $z = g/2$  and the similar equations for the second interface  $z = -g/2$ . As was explained in Ref. 1, this set of transcendental equations can be replaced by a simpler set of algebraic equations.

Let us introduce a vector of coefficients

$$X_n^N \equiv \begin{pmatrix} x_n \\ y_n \\ t_n \\ z_n \end{pmatrix}, \quad N = 1, 2, 3, 4. \quad (4.1)$$

Then the set of equations can be written in a matrix form:

$$\Sigma_N \Sigma_n A_{LN}^{nl} X_n^N = P_L^l, \quad L, N = 1, 2, 3, 4; n, l = 1, 2, \dots, \infty. \quad (4.2)$$

Eq. (4.2) constitutes an infinite system of linear algebraic equations for the unknown coefficients  $X_n^N$ .

The coefficients  $A_{LN}^{nl}$  and the right-hand sides  $P_L^l$  of the matrix eq. (4.2) for a cavity are presented in Table 1. There

$$\phi_{mn}(p) = \begin{cases} \nu_n J_0(\nu_n p) J_1(\nu_n) / (\nu_n^2 - p^2 \nu_m^2), & \text{if } \nu_n \neq p \nu_m; \\ \nu_n J_1^2(\nu_n) / (\nu_n + p \nu_m), & \text{if } \nu_n = p \nu_m. \end{cases} \quad (4.3)$$

In particular,

$$\phi_{mn}(1) = \delta_{nm} J_1^2(\nu_n) / 2. \quad (4.4)$$

For a collimator, Eq. (4.2) looks the same but its coefficients and the right-hand sides have a different meaning and are presented in Table 2.

Two geometries considered in Ref. 1 (a pipe with a sudden increase or decrease of its cross section) are particular cases of geometries considered in the present paper. For example, the case of a charge passing through a decreasing cross section can be obtained by assuming  $a_2 = b$  (or equivalently,  $p_2 = 1$ ) and  $g = 0$  in equations describing a collimator. The same case can be obtained by assuming  $a_1 = b$  (or equivalently,  $p_1 = 1$ ) and  $g = 0$  in equations describing a cavity. Similarly, the case of a charge passing through an increasing cross section can be obtained by assuming  $a_1 = b$  (or equivalently,  $p_1 = 1$ ) and  $g = 0$  in equations describing a collimator. The same case can be obtained by assuming  $a_2 = b$  (or equivalently,  $p_2 = 1$ ) and  $g = 0$  in equations describing a cavity. Using Eq. (4.4), it is easy to see that with necessary changes in notation, Eq. (4.2) indeed reduces to Eq. (12) of Ref. 1.

Notice that for a smooth pipe for which  $p_1 = p_2 = 1$  or  $q_1 = q_2 = 1$  all  $P_L^l = 0$ . Since  $\text{Det}|A_{LN}^{nl}| \neq 0$ , only the trivial solution  $X_n^N = 0$  exists. That means that there is no radiation in a smooth pipe, as it should be.

#### 5. Longitudinal Coupling Impedance

The usual expression for the longitudinal impedance is:

$$Z(k) = -\frac{2\pi}{Q} \int_{-\infty}^{\infty} dz \tilde{E}_z^R(r=0, z) \exp\{-ikz/\beta\}, \quad (5.1)$$

where  $E_z^R$  is the radiative part of the field, i.e., the part which depends on the expansion coefficients. Sometimes an alternative definition of the impedance is used in which the integration is performed over the difference between the full field and the field of a charge in a smooth pipe. This definition is useful only if both side pipe cross sections have equal radii  $a_1 = a_2 = a$  or, equivalently,  $p_1 = p_2 = p$ . In this case the real parts of the impedance are the same according to both definitions. The imaginary parts differ by

$$\Delta Z = -iZ_0 \kappa \tilde{g} F(a) / \pi \gamma^2 \beta^2, \quad (5.2)$$

where  $4\pi/c = Z_0 = 377 \Omega$  is the impedance of free space and  $F(a)$  is defined in Table 1. In the general case of different pipe radii, definition (5.1) is more useful and is used below.

Table 1. Coefficients  $A_{LN}^{nl}$  and right-hand sides  $P_L^l$  of Eq. (4.2) for a cavity

$$E_+ = \exp\{2i\tilde{g}(\kappa/\beta + \tilde{\lambda}_{bn})\}, \quad E_- = \exp\{-2i\tilde{g}(\kappa/\beta - \tilde{\lambda}_{bn})\}, \quad F(a) = K_0(\tau b)/I_0(\tau b) - K_0(\tau a)/I_0(\tau a)$$

$$p_1 = a_1/b, \quad p_2 = a_2/b, \quad \tilde{g} = g/2b$$

$N$ $L$	1	2	3	4	
1	$2p_1^2 \tilde{\lambda}_{a1n} \phi_{ln}(p_1)$	$\tilde{\lambda}_{bn} J_1^2(\nu_n) \delta_{nl}$	$-\tilde{\lambda}_{bn} J_1^2(\nu_n) \delta_{nl} E_+$	0	$J_0(\nu_1 p_1)/I_0(\tau a_1)(\nu_1^2 + (\tau b)^2)$
2	$\nu_n^2 J_1^2(\nu_n) \delta_{ln}$	$-2p_1^2 \nu_n^2 \phi_{nl}(p_1)$	$-2p_1^2 \nu_n^2 \phi_{nl}(p_1) E_+$	0	$-(\tau b) p_1^2 \nu_1 J_1(\nu_1) I_0(\tau a_1) F(a_1)/(\nu_1^2 + (\tau a_1)^2) \gamma$
3	0	$\tilde{\lambda}_{bn} J_1^2(\nu_n) \delta_{nl} E_-$	$-\tilde{\lambda}_{bn} J_1^2(\nu_n) \delta_{nl}$	$2p_2^2 \tilde{\lambda}_{a2n} \phi_{ln}(p_2)$	$J_0(\nu_1 p_2)/I_0(\tau a_2)(\nu_1^2 + (\tau b)^2)$
4	0	$-2p_2^2 \nu_n^2 \phi_{nl}(p_2) E_-$	$-2p_2^2 \nu_n^2 \phi_{nl}(p_2)$	$-\nu_n^2 J_1^2(\nu_n) \delta_{ln}$	$-(\tau b) p_2^2 \nu_1 J_1(\nu_1) I_0(\tau a_2) F(a_2)/(\nu_1^2 + (\tau a_2)^2) \gamma$

Performing the integration in formula (5.1) we find:

$$Z(k) = -(Z_0/\pi) \Sigma_n \left\{ x_n(\kappa/\beta - \tilde{\lambda}_{a1n}) / [1 + (\tau a_1/\nu_n)^2] \right.$$

$$+ y_n(\kappa/\beta + \tilde{\lambda}_b) (\exp\{2i\tilde{g}(\tilde{\lambda}_b - \kappa/\beta)\} - 1) / [1 + (\tau b/\nu_n)^2]$$

$$- t_n(\kappa/\beta - \tilde{\lambda}_b) (\exp\{2i\tilde{g}(\tilde{\lambda}_b + \kappa/\beta)\} - 1) / [1 + (\tau b/\nu_n)^2]$$

$$\left. + z_n(\kappa/\beta + \tilde{\lambda}_{a2n}) / [1 + (\tau a_2/\nu_n)^2] \right\} . \quad (5.3)$$

Formula (5.3) is valid for both a cavity and a collimator. The expansion coefficients  $x_n, y_n, t_n,$  and  $z_n$  in this formula should be understood as solutions of corresponding equations for a cavity and a collimator, respectively.

In the ultrarelativistic limit  $\gamma \rightarrow \infty$  there is an alternative way of calculating the impedance for a cavity with equal side pipes radii. Instead of integrating the field along the axis of the structure  $r = 0$  one can as well integrate the field along any line  $r = R$ :<sup>6,7</sup>

$$Z_R(k) = -\frac{2\pi}{Q} \int_{-\infty}^{\infty} dz \tilde{E}_z(r = R, z) \exp(-ikz) . \quad (5.4)$$

Performing the integration we find:

$$Z_R(k) = -(Z_0/\pi) \Sigma_n \left\{ x_n J_0(\nu_n R/a) (\kappa - \tilde{\lambda}_{a1n}) \right.$$

$$+ y_n J_0(\nu_n R/b) (\kappa + \tilde{\lambda}_b) \left[ \exp\{2i\tilde{g}(\tilde{\lambda}_b - \kappa)\} - 1 \right]$$

$$- t_n J_0(\nu_n R/b) (\kappa - \tilde{\lambda}_b) \left[ \exp\{2i\tilde{g}(\tilde{\lambda}_b + \kappa)\} - 1 \right]$$

$$\left. + z_n J_0(\nu_n R/a) (\kappa + \tilde{\lambda}_{a2n}) \right\} . \quad (5.5)$$

A remarkable feature of this formula is that the right-hand side of it *does not* depend on  $R$  in spite of its explicit presence there.

In particular for a cavity, a convenient choice is  $R = a$ . Due to the boundary condition (3.1) the regions  $z > g/2$  and  $z < -g/2$  do not contribute to the value of the integral.

Table 2. Coefficients  $A_{LN}^{nl}$  and right-hand sides  $P_L^l$  of Eq. (4.2) for a collimator

$$E_+ = \exp\{2i\tilde{g}(\kappa/\beta + \tilde{\lambda}_{bn})\}, \quad E_- = \exp\{-2i\tilde{g}(\kappa/\beta - \tilde{\lambda}_{bn})\}, \quad F(a) = K_0(\tau b)/I_0(\tau b) - K_0(\tau a)/I_0(\tau a)$$

$$q_1 = b/a_1, \quad q_2 = b/a_2, \quad \tilde{g} = g/2b$$

$N$ $L$	1	2	3	4	
1	$\tilde{\lambda}_{a1n} J_1^2(\nu_n) \delta_{nl}$	$2q_1^2 \tilde{\lambda}_{bn} \phi_{ln}(q_1)$	$-2q_1^2 \tilde{\lambda}_{bn} \phi_{ln}(q_1) E_+$	0	$-J_0(\nu_1 q_1)/I_0(\tau a_1)(\nu_1^2 + (\tau b)^2)$
2	$2q_1^2 \nu_n^2 \phi_{nl}(q_1)$	$-\nu_n^2 J_1^2(\nu_n) \delta_{ln}$	$-\nu_n^2 J_1^2(\nu_n) \delta_{ln} E_+$	0	$-(\tau b) q_1^2 \nu_1 J_1(\nu_1) I_0(\tau a_1) F(a_1)/(\nu_1^2 + (\tau a_1)^2) \gamma$
3	0	$2q_2^2 \tilde{\lambda}_{bn} \phi_{ln}(q_2) E_-$	$-2q_2^2 \tilde{\lambda}_{bn} \phi_{ln}(q_2)$	$\tilde{\lambda}_{a2n} J_1^2(\nu_n) \delta_{nl}$	$-J_0(\nu_1 q_2)/I_0(\tau a_2)(\nu_1^2 + (\tau b)^2)$
4	0	$-\nu_n^2 J_1^2(\nu_n) \delta_{ln} E_-$	$-\nu_n^2 J_1^2(\nu_n) \delta_{ln}$	$-2q_2^2 \nu_n^2 \phi_{nl}(q_2)$	$-(\tau b) q_2^2 \nu_1 J_1(\nu_1) I_0(\tau a_2) F(a_2)/(\nu_1^2 + (\tau a_2)^2) \gamma$

Putting  $R = a$  in Eq. (5.5) yields,

$$Z_{cav}(k) = - (Z_0/\pi) \sum_n J_0(\nu_n p) \left\{ y_n(\kappa + \tilde{\lambda}_b) \left[ \exp\{2i\tilde{g}(\tilde{\lambda}_b - \kappa)\} - 1 \right] - t_n(\kappa - \tilde{\lambda}_b) \left[ \exp\{2i\tilde{g}(\tilde{\lambda}_b + \kappa)\} - 1 \right] \right\} \quad (5.6)$$

For a collimator, a convenient choice is  $R = b$ . In this case due to boundary condition (3.1) the region  $-g/2 < z < g/2$  does not contribute to the value of the integral and we obtain ( $q_1 = b/a_1, q_2 = b/a_2$ ):

$$Z_{coll}(k) = - (Z_0/\pi) \sum_n \left[ x_n J_0(\nu_n q_1)(\kappa - \tilde{\lambda}_b) + z_n J_0(\nu_n q_2)(\kappa + \tilde{\lambda}_b) \right] \quad (5.7)$$

For large  $\gamma$  the impedances obtained by means of all the formulae (5.3), (5.5), (5.6) and (5.7) agree very well and this feature is used as a check in numerical codes.

## 6. Numerical Results and Conclusion

In general, the solution of Eq. (4.2) can be found only numerically. Two computer codes, RCVTY (for the geometry sketched in Fig. 1a) and RCLMTR (for the geometry sketched in Fig. 1b), have been written for this purpose. An approximate solution is found by truncating the matrix to a finite size, inverting it and solving for the coefficients. In a normal case, *i.e.*, not for extreme values of parameters, a matrix size of  $20 \times 20$  is usually sufficient to obtain reasonable accuracy. The results are checked to be independent on the matrix size up to the maximum size of  $100 \times 100$  allowed by the codes. The programs, if asked, can do an additional check for the correctness of the solution. Namely, the coefficients found are used to restore the continuity and the boundary conditions at the interfaces between different cylindrical regions.

As an illustration of the results obtained with the help of RCVTY the real and imaginary parts of the longitudinal impedance for a cavity with the same dimensions as used in Ref. 2 are represented in Figs. 2 and 3, respectively. The plots are in good agreement with the result of that paper for all the frequencies except those around the cut-off frequencies of the pipe  $ka = 2.405$ .

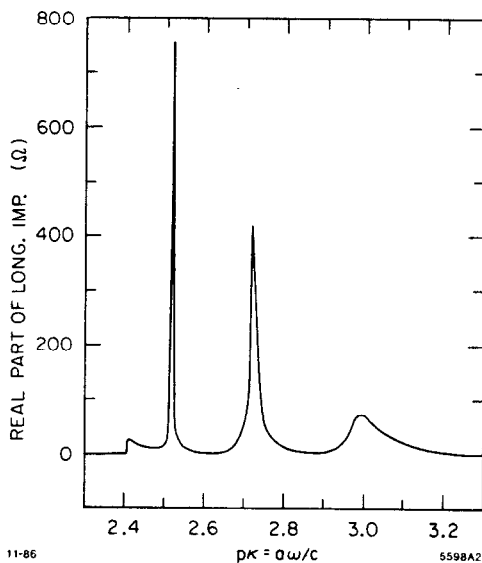


Fig. 2. Real part of the longitudinal impedance of a cavity as function of dimensionless frequency  $p\kappa = a\omega/c$ .  $a = a_1 = a_2$ ,  $g/2b = 0.302$ ,  $a/b = 0.152$ .

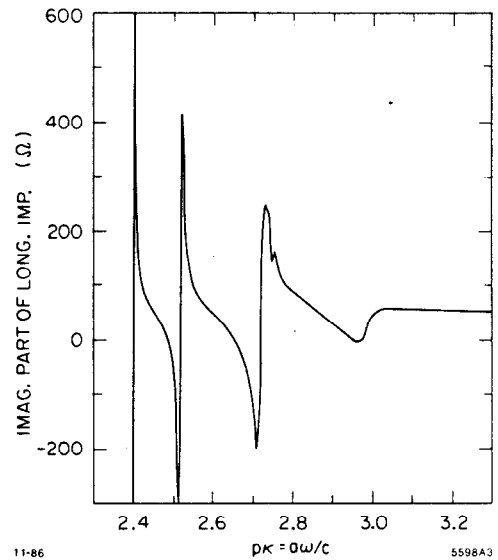


Fig. 3. The same as in Fig. 2 but for the imaginary part of the impedance.

Dependence of the impedance on the charge energy is illustrated in Figs. 4 and 5. Here the real and imaginary parts of the longitudinal impedance of a cavity are plotted for several different Lorentz factors  $\gamma$ . As one can see, from the point of view of the impedance  $\gamma = 5$  is already close enough to  $\infty$ ,  $\gamma = 10$  is indistinguishable from  $\infty$ .

The real and imaginary parts of the impedance of a very thin cavity built out of two pipe flanges and a vacuum edge electrically connecting them are plotted in Figs. 6 and 7, respectively.

To illustrate the results obtained with the help of RCLMTR the real and imaginary parts of the impedance of a washer in a pipe (thin collimator) for the SLAC geometry are plotted in Figs. 8 and 9, respectively.

The impedance of a long collimator can be seen as the sum of two impedances for a sudden increase and decrease of the pipe cross section. The impedance in the range of

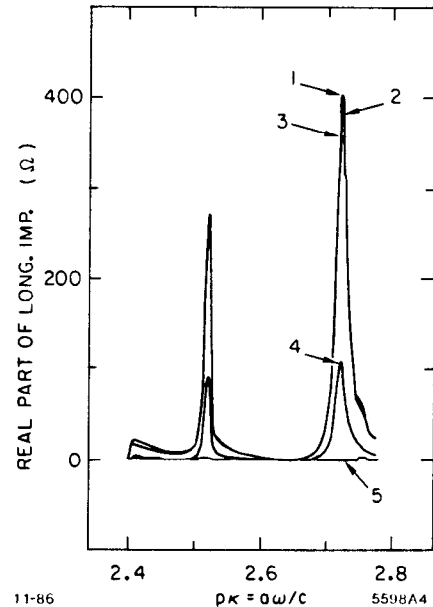


Fig. 4. Illustration of the dependence of the real part of the impedance on  $\gamma$  for the same cavity as in Fig. 2. 1)  $\gamma = 100$ , 2)  $\gamma = 10$ , 3)  $\gamma = 5$ , 4)  $\gamma = 2$ , 5)  $\gamma = 1.4$ .

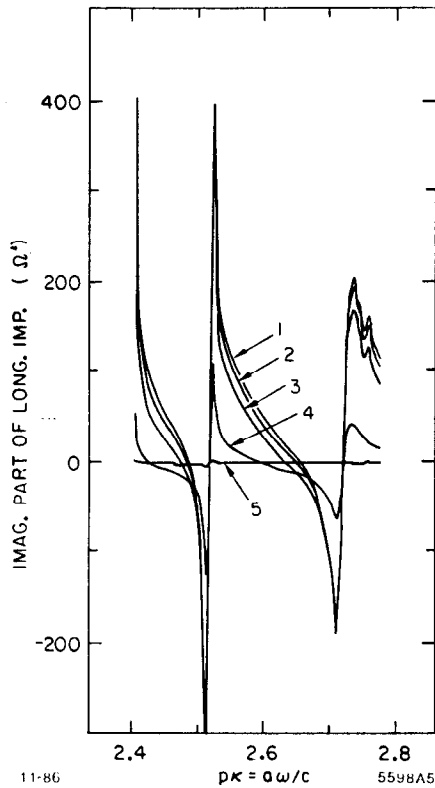


Fig. 5. The same as in Fig. 4 but for the imaginary part of the impedance.

large frequencies, found using formula (5.7), coincides with the impedance of a sudden *increase* of the pipe cross section found in the paper.<sup>1</sup> This is the consequence of the fact that the impedance of a sudden *decrease* of the pipe cross section tends to zero for large frequencies.

An analytic derivation of the asymptotic formula for the impedance of a collimator is presented in the Appendix. As is discussed there the impedance is constant in the frequency range  $\kappa < \gamma$  and then falls down.

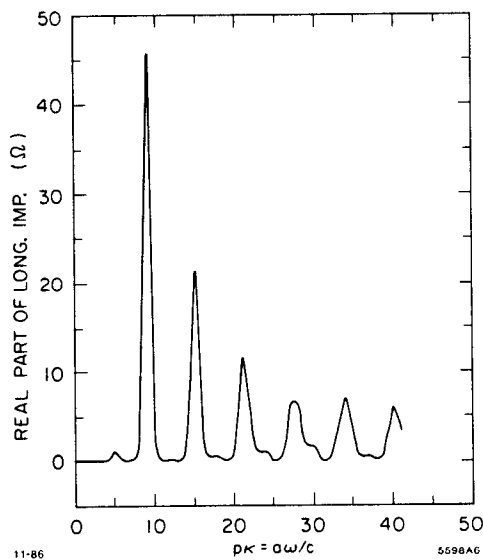


Fig. 6. Real part of the longitudinal impedance of a very thin cavity (e.g., built of flanges) as function of dimensionless frequency  $\rho\kappa = a\omega/c$ .  $a = a_1 = a_2$ ,  $g/2b = 0.025$ ,  $a/b = 0.5$ .

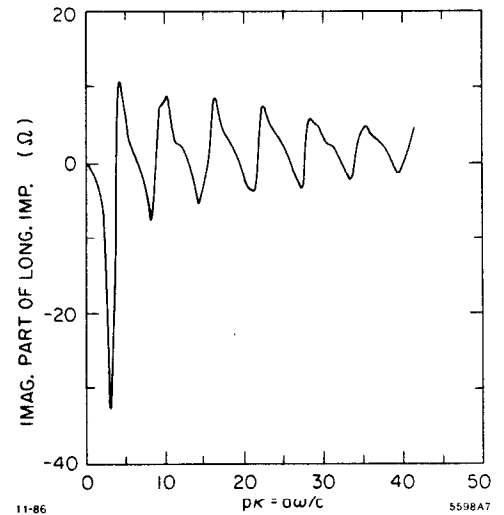


Fig. 7. The same as in Fig. 6 but for the imaginary part of the impedance.

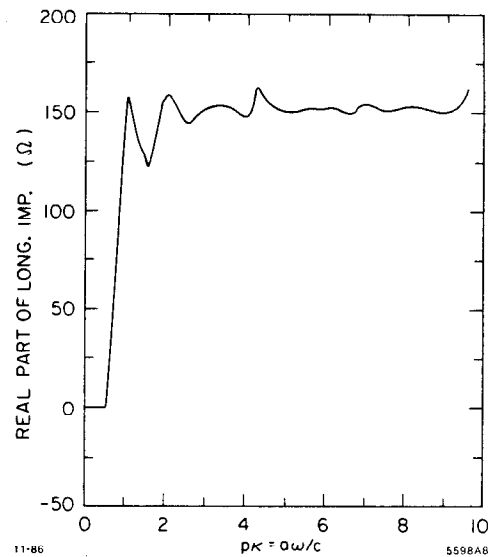


Fig. 8. Real part of the longitudinal impedance of a washer in a pipe (the SLAC type of the structure) as function of dimensionless frequency  $\rho\kappa = a\omega/c$ .  $a = a_1 = a_2$ ,  $g/2b = 0.217$ ,  $a/b = 0.281$ .

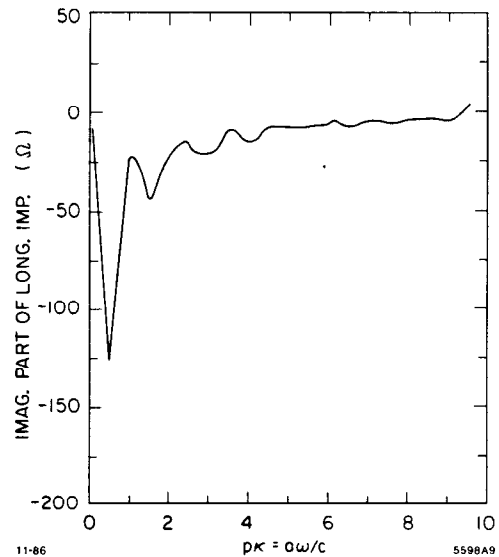


Fig. 9. The same as in Fig. 8 but for the imaginary part of the impedance.

It is interesting to estimate the total energy loss  $\Delta W$  of a distributed charge passing through a collimator:

$$\Delta W = \int_{-\infty}^{\infty} d\omega |f(\omega)|^2 \operatorname{Re} Z_{coll}(k) , \quad (6.1)$$

where  $f(\omega)$  is the Fourier transform of the charge density. Let us assume  $f(\omega)$  to be Gaussian:

$$f(\omega) = (Q/2\pi) \exp(-k^2 \sigma^2 / 2) , \quad (6.2)$$

where  $\sigma$  is rms of the longitudinal charge distribution.

If one assumes that  $\operatorname{Re} Z_{coll}$  is constant and given by Eq. (A.6) then the total energy loss is

$$\Delta W = \frac{Q^2}{\pi^{3/2} \sigma} \ln a/b . \quad (6.3)$$

This expression is valid when  $\sigma > b/\gamma$  and agrees with formula for the total energy loss of a charge passing through a sudden change in a pipe cross section obtained in the paper.<sup>11</sup>

For a point charge  $\sigma = 0$ . If one assumes that  $\operatorname{Re} Z_{coll}$  is constant for  $\kappa < \gamma$  and is zero for  $\kappa > \gamma$ , as was discussed above, then the total energy loss is proportional to  $\gamma$ . That conclusion is in agreement with an estimate<sup>8</sup> and numerical calculations<sup>9, 10</sup> for a charge passing through a hole in a screen.

#### Acknowledgements

The author is grateful to K. Bane and S. Heifets for many useful discussions and comments, and to B. Woo for the help with numerical calculations.

#### Appendix: Asymptotic Formula for the Impedance of a Collimator

The longitudinal impedance of a collimator in the large frequency domain (and for the relativistic case  $\gamma \gg 1$ ) can be found analytically. We will do that using formula (5.7). Since asymptotically  $\tilde{\lambda}_b \approx \kappa$ , only the diffracted field, i.e., the field depending on coefficients  $z_n$ , contributes to the impedance. Physically that arises from the fact that only the diffracted field radiated ahead can reach the relativistic particle. Hence,

$$Z_{coll}(k) = -2(Z_0/\pi) \kappa \sum_n z_n J_0(\nu_n q) , \quad (A.1)$$

where  $q = a/b$ ,  $a$  and  $b$  are the exit pipe and collimator radii, respectively.

The coefficients  $z_n$  can be found from Eq. (4.2) with the matrix and the right-hand side of it taken from Table 2:

$$z_l \kappa J_1^2(\nu_l) = -J_0(\nu_l q) / \nu_l^2 + 2q^2 \kappa \sum_m (t_m - y_m E_-) \phi_{lm} , \quad (A.2)$$

where the quantities  $\phi_{lm}$  are defined in Eq. (4.3). Divide now Eq. (A.2) by  $J_1^2(\nu_l)$ , multiply by  $J_0(\nu_l q)$  and sum over  $l$ :

$$\begin{aligned} \kappa \sum_l z_l J_0(\nu_l q) &= -\sum_l J_0^2(\nu_l q) / \nu_l^2 J_1^2(\nu_l) \\ &+ 2\kappa \sum_l J_0(\nu_l q) J_1^2(\nu_l)^{-2} \\ \sum_m (t_m - y_m E_-) \nu_m J_1(\nu_m) (\nu_m^2 / q^2 - \nu_l^2)^{-1} &. \end{aligned} \quad (A.3)$$

Summation here can be performed explicitly using the following particular form of the Kneser-Sommerfeld formula:<sup>12</sup>

$$\begin{aligned} \sum_l J_0^2(\nu_l q) (\nu_l^2 - x^2)^{-1} J_1^{-2}(\nu_l) \\ = \pi J_0(qx) \{ J_0(qx) Y_0(x) - J_0(x) Y_0(qx) \} / 4J_0(x) , \end{aligned} \quad (A.4)$$

where  $Y_0$  is Bessel function of the second kind.

One can easily see that the second term containing coefficients  $t_m$  and  $y_m$  vanishes. First, interchange the order of the summations over  $l$  and  $m$ . Then formula (A.4) applies with  $x = \nu_m/q$  and the result of summation is zero.

Application of the same formula with  $x \rightarrow 0$  to the first sum in Eq. (A.3) gives:

$$\begin{aligned} \sum_l J_0^2(\nu_l q) / \nu_l^2 J_1^2(\nu_l) &= -\pi \lim_{x \rightarrow 0} [Y_0(x) - Y_0(px)] \\ &= (\ln q) / 2 . \end{aligned} \quad (A.5)$$

Hence, for large energy and for large frequencies the impedance of a collimator is the following constant:

$$Z_{coll}(\kappa) = (Z_0/\pi) \ln(a/b) \quad \text{for } \kappa \gg 1, \gamma \gg 1 . \quad (A.6)$$

From this formula it may seem that the corresponding wake field, which is the Fourier transform of the impedance, diverges at the zero distance behind the charge. That is not necessarily true. Indeed, derivation of this formula is based on the approximate Eq. (5.7) which is valid in the limit  $\gamma \gg \kappa$ . Comparing Eq. (5.7) and the exact Eq. (5.3) one can conclude that formula (A.6) is not valid for  $\kappa > \gamma$ . In this range of frequencies impedance should decrease at least as  $k^{-2}$ .

#### References

1. S. A. Kheifets, S. A. Heifets, *Radiation of a Charge in a Perfectly Conducting Cylindrical Pipe with a Jump in its Cross Section*, Proc. of Lin. Accel. Conf., SLAC-REPORT-303, p. 493, Sept. 1986; SLAC-PUB-3965, May 1986.
2. H. Henke, *Point Charge Passing a Resonator with Beam Tubes*, CERN-LEP-RF/85-41, CERN, Geneva, Switzerland, Nov. 1985.
3. S. Kheifets, J. Jaeger and S. Yu, *IEEE-Microwave Theory*, Vol. MTT-33, No. 6, p. 467, June 1985.
4. See, e.g., S. Kheifets and B. Zotter, *Nucl. Instr. and Methods*, **A243**, p. 13-27, 1986.
5. J. A. Stratton, *Electromagnetic Theory*, N. Y., McGraw-Hill, 1941.
6. T. Weiland, *Nucl. Instr. and Methods*, **216**, 31, (1983).
7. B. Zotter and K. Bane, *Transverse Resonances of Periodically Widened Cylindrical Tubes with Circular Cross Section*, PEP-Note 308, SLAC, Sept. 1979.
8. J. D. Lowson, Report RHEL M144, Rutherford Laboratory, 1968 (unpublished).
9. Yu. N. Dnestrovskii and D. P. Kostomarov, *Soviet Physics -Doklady*, **124**, No. 1, p. 132 (1959).
10. Yu. N. Dnestrovskii and D. P. Kostomarov, *Soviet Physics -Doklady*, **124**, No. 1, p. 158 (1959).
11. V. E. Balakin and A. V. Novokhatsky, *Proc. of the 12th Intern. Conf. on High-Energy Accel., Fermilab, August 11-16, 1983*, p. 117.
12. *Higher Transcendental Functions*, Vol. II, p. 104, McGraw-Hill, 1953.